The origin of the conductivity maximum in molten salts. I. Bismuth chloride

Adam T. Clay, Colin M. Kuntz, Keith E. Johnson, and Allan L. L. East

Citation: J. Chem. Phys. **136**, 124504 (2012); doi: 10.1063/1.3694830
View online: http://dx.doi.org/10.1063/1.3694830
View Table of Contents: http://jcp.aip.org/resource/1/JCPSA6/v136/i12
Published by the American Institute of Physics.

The origin of the conductivity maximum in molten salts. I. Bismuth chloride

Adam T. Clay,[a] Colin M. Kuntz, Keith E. Johnson, and Allan L. L. East[b]
Department of Chemistry and Biochemistry, University of Regina, Regina, Saskatchewan S4S 0A2, Canada

(Received 25 November 2011; accepted 29 February 2012; published online 26 March 2012)

A new theory is presented to explain the conductivity maxima of molten salts (versus temperature and pressure). In the new theory, conductivity is due to ions hopping from counterion to counterion, and its temperature dependence can be explained with an ordinary Arrhenius equation in which the frequency prefactor *A* (for hopping opportunities) and activation energy E_a (for hopping) are density dependent. The conductivity maximum is due to competing effects: as density decreases, the frequency of opportunities for hopping increases, but the probability that an opportunity is successfully hopped decreases due to rising E_a caused by the increased hopping distance. The theory is successfully applied to molten bismuth (III) chloride, and supported by density-functional based molecular dynamics simulations which not only reproduce the conductivity maximum, but disprove the long-standing conjecture that this liquid features an equilibrium between $BiCl_3$ molecules, and $BiCl_2^+$ and $BiCl_4^-$ ions that shifts to the left with increasing temperature. © *2012 American Institute of Physics*. [http://dx.doi.org/10.1063/1.3694830]

I. INTRODUCTION

Modern ionic liquids have potential as non-aqueous electrolytes,[1] but improved understanding of their mechanisms of electrical conductivity is needed. One issue thought to be understood was the origins of conductivity maxima of simple molten salts (versus PVT variables), a phenomenon discovered by Grantham and Yosim in the 1960's.[2–5] Bismuth (III) chloride played a special role in the development of a theory to explain this phenomenon, because its conductivity maximum is relatively easy to reach in the laboratory (425 °C),[2] and because the conductivity can be reduced by several orders of magnitude near supercritical temperatures.[5,6] Grantham and Yosim's original hypothesis was that the loss of conductivity at higher temperatures is due to increased ion association as density falls. This hypothesis was supported by Tödheide, who incorporated a degree of ionization α into the theory, assumed for $BiCl_3$ an ionic equilibrium of $2BiCl_3 \leftrightarrows BiCl_2^+ + BiCl_4^-$, and used monotonically increasing ion mobilities with temperature to show that the conductivity maximum can be explained with α values that steadily decrease as the density falls during orthobaric heating.[6,7] Raman and neutron-scattering studies have been inconclusive on the nature of the ions present.[8–11] The purpose of this paper is to show that Tödheide's assumptions appear to be incorrect, and that the conductivity maximum can be explained with an *ordinary Arrhenius equation* having density-dependent parameters justifiable with a model of atomic ions.

In the degree-of-ionization theory of Tödheide,[7] one starts with a general formula for the specific conductivity σ due to mobile ions

$$\sigma = \sum_i \rho_i |z_i e| \mu_i, \tag{1}$$

where ρ_i, $z_i e$, and μ_i are the number density, charge, and conventional mobility (units C s kg^{-1}) of ion type *i*, respectively. To incorporate a degree of ionization α for partly ionized liquids, Tödheide wrote

$$\rho_i = \nu_i \alpha \rho_0 = \nu_i \alpha N_{AVO} / V_m, \tag{2}$$

where ρ_0 is the number density of the molecules when the salt is completely unionized, ν_i is a stoichiometric coefficient, N_{AVO} is Avogadro's number, and V_m is the molar volume. This leads to

$$\sigma = \alpha (N_{AVO} / V_m) \sum_i \nu_i |z_i e| \mu_i \tag{3}$$

in which Tödheide points out that PVT dependence can be in any of V_m, μ_i, and α. One also defines a molar conductivity $\Lambda \equiv \sigma V_m$, and hence,

$$\Lambda = \alpha N_{AVO} \sum_i \nu_i |z_i e| \mu_i \tag{4}$$

in which the PVT dependence is only in μ_i and α.

Equations (3) and (4) appeared to be sufficient to explain observed phenomena. For fully ionized systems where $\alpha = 1$, the PVT dependence of molar conductivity of the fully ionized liquid would lie entirely in the mobilities, and this agrees with experimental observations for molten alkali halides (except lithium halides), for which molar conductivity rises with T (constant p), and falls with p (constant T). The dependence on temperature is nicely modelled by the Arrhenius law

$$\Lambda = A e^{-E_a / RT} \tag{5}$$

for these molten salts, since plots of ln Λ vs. 1/T are linear. Specific conductivity σ also rises with T (constant p) for these alkali halides.[12]

[a] Present address: Department of Molecular and Cellular Biology, University of Guelph, Guelph, Ontario N1G 2W1, Canada.
[b] Author to whom correspondence should be addressed: allan.east@uregina.ca.

Equations (3) and (4) also nicely explained the conductivity maximum versus T at mild pressures that had been observed in other metal halide melts such as $BiCl_3$. Bismuth chloride has a melting point of 232 °C,[13] a normal boiling point of 442 °C,[14] and a critical point of 905 °C.[15] Yosim and co-workers studied the dependence of molten $BiCl_3$ conductivity upon T, but along the more convenient "orthobaric" liquid/vapour coexistence curve rather than at constant p or V. This procedure allowed them to collect data over a larger liquid range than could be done at atmospheric pressures (initially 230–630 °C,[2] and later up to 960 °C[4]). They found a maximum in σ at 425 °C, and a maximum in Λ at 460 °C (Ref. 2) later corrected to 475 °C.[15] Since molar volume does not appear in Eq. (4), these maxima were ascribed to competing effects of μ vs. α: if mobility is increasing in the 400–500 °C range, then α *must be decreasing*, i.e., the degree of ionization must be falling. This Yosim hypothesis (later formalized by Tödheide) was supported by Johnson and Cubicciotti,[15] who measured orthobaric densities of $BiCl_3$ beyond the normal boiling point and identified their temperature dependence as behaving like those of a molecular fluid. Also, this decrease in α at high T is a phenomenon known to cause similar maxima in the conductivity of aqueous electrolytes.[16,17]

To this day, this hypothesis of a decreasing degree of ionization of $BiCl_3$ versus T has had no apparent holes. We hoped to observe this shift in equilibrium by undertaking a series of *ab initio* molecular dynamics (AIMD) simulations of molten $BiCl_3$ at a variety of temperatures and densities. The results here reproduce the conductivity maximum under orthobaric conditions, but in these simulations Cl ions have coordination numbers of 2, not 1, and thus the Tödheide equilibrium now appears to be incorrect. In this report, we provide evidence that the degree of ionization approach of Tödheide is not satisfactory for $BiCl_3$, and instead assign the conductivity maximum to a maximum in *relative* ion mobility, best understood as a product of two competing mobility effects that vary with liquid density. This is a fundamental change to the theory of conductivity in molten $BiCl_3$ and may find broader application.

II. THEORETICAL METHODS

Simulations were performed using the Vienna *ab initio* simulation package (VASP) software,[18,19] using its potpawGGA plane-wave basis sets,[20,21] standard precision (PREC = NORMAL), ENMAX = 400 eV, a Nosé thermostat for canonical-ensemble (NVT) conditions[22] with 40 fs thermal oscillations (SMASS = 0), and a Verlet velocity algorithm[23] with time step τ = 4 fs. The cubic simulation cell consisted of $Bi_{16}Cl_{48}$ and was replicated using periodic boundary conditions to mimic the bulk liquid. Simulations typically went for 1000 steps (4 ps) for equilibration, and then 54 000 steps (216 ps) for sampling.

For forces the PW91 level of density functional theory[24] was used, but with an added, Grimme-style,[25] semiempirical van der Waals (vdW) attractive potential, because our initial simulations in 2008 and 2010 without this vdW potential seemed more solid-like than liquid-like at 240 °C and 330 °C, temperatures past the true melting point. Grimme parameters for bismuth were taken to be C_6 = 63.55 J nm^6 mol^{-1} and R_0 = 1.9 Å; the former was calculated using the same UPBE0/QZVP recipe Grimme used (we practiced this by reproducing Grimme's value for P atom), and the latter was taken to be the same as Grimme used for Sb, the element above it in the periodic table, due to the lanthanide contraction rule.

Equilibration testing was performed using high-temperature simulations (T = 580 °C, cell width 13.91 Å, time 16 ps) with different starting atomic arrangements. The "ionic" set began with a random array of eight $BiCl_2^+$ and eight $BiCl_4^-$ ions, while the "molecular" set began with 16 pyramidal $BiCl_3$ molecules in a regular array. A third "random" set began from an already equilibrated geometry from an old set of data from 2010 whose simulation did not employ the added Grimme's potential. Each simulation equilibrated at around 4 ps of simulation time, converging both structurally and energetically to a common structure of atomic ions. Hence we were free to start with any of these equilibrated samples. The relative cell positions ("direct" coordinates) of the atoms at the final time step of the molecular array run were used as the starting positions for all ensuing runs. The energies of the orthobaric production runs were also monitored and found to be equilibrated throughout the sample time (Fig. 1).

Two sets of production runs were performed. The main set was performed at six (ρ,T) points mimicking Yosim's original orthobaric experimental conditions:[2] six temperatures were chosen from 260 to 660 °C in 80° intervals, and the densities were taken according to the density function

$$\rho(\mathrm{g\,mL^{-1}}) = 5.073 - 0.0023\,\mathrm{T\,(K)}, \tag{6}$$

which was summarized by Janz[26] from fits of experimental data for the temperature range of 250–350 °C. The function also fits well (within 3%) the orthobaric ρ data determined in the 500–700 °C range by Johnson and Cubicciotti,[15] and hence is appropriate throughout the temperature range of interest. The simulations beyond the normal boiling point correspond to raised-pressure, sub-critical liquids. The second set of production runs were designed to apportion changes in conductivity to either changes in density or in temperature,

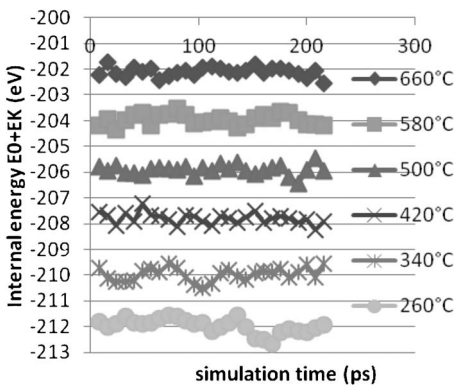

FIG. 1. Energy stability monitoring plots from AIMD simulations. Each point is an average of the energies of 2000 consecutive steps.

via simulations that held either the density or the temperature constant.

Diffusion coefficients D_{Bi} and D_{Cl} and specific conductivity σ were computed via both Einstein and Green-Kubo formulae. The Green-Kubo formulae employed were

$$D_X^{GK} = \frac{1}{3}\left\langle\left\langle \vec{v}_{X,i}^2(t_0)\right\rangle\right\rangle \int_{t=0}^{\infty} \tilde{C}_{X,i}(t;t_0)dt, \tag{7}$$

where

$$\tilde{C}_{X,i}(t;t_0) = \frac{\langle\langle \vec{v}_{X,i}(t)\cdot\vec{v}_{X,i}(t_0)\rangle\rangle}{\langle\langle \vec{v}_{X,i}^2(t_0)\rangle\rangle}, \tag{8}$$

$$\sigma^{GK} = \rho_n \Theta \int_{t=0}^{\infty} \tilde{C}_J(t;t_0)dt, \tag{9}$$

where

$$\tilde{C}_J(t;t_0) = \frac{\langle \vec{j}(t)\cdot\vec{j}(t_0)\rangle}{\langle \vec{j}^2(t_0)\rangle}, \tag{10}$$

$$\vec{j}(t) = \sum_i^{Nions} z_i e \vec{v}_i(t), \tag{11}$$

$$\Theta = z_A z_B e^2 \left(\frac{z_B}{m_B} - \frac{z_A}{m_A}\right). \tag{12}$$

In Eqs. (7) and (8), $C_{X,i}(t;t_0)$ is the normalized velocity autocorrelation function for ion i of type X, $\vec{v}_{X,i}(t)$ is the instantaneous velocity of ion i of type X at time t, and the brackets denote averaging over all ions i of type X, and over all choices of time zero t_0.[23] In Eqs. (9)–(12), ρ_n is the number density (m^{-3}) of A_xB_y (here $BiCl_3$) formula units in the simulation cell, Θ is a charge/mass factor (for $BiCl_3$ $z_A = +3$, $z_B = -1$, and $\Theta = 1.974 \times 10^{-12}$ C^2/kg), $\vec{j}(t)$ is the instantaneous current in the simulation cell at time t, e is the proton charge (1.60218×10^{-19}C), and $\tilde{C}_J(t;t_0)$ is the normalized current autocorrelation function, averaged only over the choices of time zero t_0 since current is a collective property. Equation (9) is derived in the Appendix. The Einstein formulae used were

$$D_X^{Ein} = \lim_{t\to\infty} \frac{\langle\langle |\vec{r}_{X,i}(t) - \vec{r}_{X,i}(t_0)|^2\rangle\rangle}{6t}, \tag{13}$$

$$\sigma^{Ein} = \frac{3\rho_n\Theta}{\langle \vec{j}^2(t_0)\rangle} \lim_{t\to\infty} \frac{\langle |\vec{M}(t) - \vec{M}(t_0)|^2\rangle}{6t}, \tag{14}$$

Here $\vec{r}_{X,i}(t)$ is the Cartesian position of the ith atom of type X at time t, and $\vec{M}(t)$ is the total electric dipole of the simulation cell at time t. The brackets indicate averaging as before, and Eq. (14) is derived in the Appendix.

We also tested the Nernst-Einstein approximation[27]

$$\sigma^{NE} \approx \frac{(N_{AVO}e)^2}{V_m RT}\left(z_A^2 \nu_A D_A + z_B^2 \nu_B D_B\right) \tag{15}$$

to demonstrate its complete breakdown at high temperatures; in this equation ν_A and ν_B are the stoichiometric coefficients of the ions (1 and 3 for Bi and Cl, respectively). A referee suggested that we also list computed Haven ratios ($H = \sigma^{NE}/\sigma^{true}$),[28] which, like Watanabe's[29,30] $\Lambda^{true}/\Lambda^{NMR}$ (which is essentially 1/H (Ref. 31) for liquids) and Hansen and McDonald's Δ,[32] are a measure of the error of this approximation. The Nernst-Einstein approximation assumes ion motions are uncorrelated, and if true H = 1. However, Haven ratios are less than one for ionic solids, due to common-ion correlation,[28] and greater than one for ionic liquids, due to opposing-ion correlation.[31,33] Some, e.g., Watanabe, have used these deviations from Nernst-Einstein "ideality" to define an effective "ionicity" of a liquid for the purposes of electrolyte assessment.[30,34]

For Green-Kubo calculations, the numerical integration from 0 to "infinity" was performed by recording running integral values via Simpson's rule every 50 timesteps ($t_f = 50\ \tau$, $100\ \tau$, ...,), and averaging all such values starting from $t_f = 1000\ \tau$ (4 ps). This averaging was done to improve precision, as the autocorrelation functions (particularly $\tilde{C}_J(t)$) were somewhat noisy due to the limited sampling possible with the AIMD technique (Fig. 2). Due to the need to also average over a number of choices of t_0 (say, n_{zero}) to improve the quality of the correlation functions before integration, the integration range (n_{inf}) could not be the full 54 000 timesteps: the choices of (n_{zero}, n_{inf}) we tried were (8k, 46k), (18k, 36k), (28k, 26k), (38k, 16k). Note $\tau = 4$ fs, and hence integrals out to $46 \times 4 = 184$ ps were done on low-quality functions and out to $16 \times 4 = 64$ ps on our highest-quality functions.

For Einstein calculations, the extrapolation to infinity of the relevant function in Eqs. (13) or (14) was performed by recording values of the function every 25 timesteps, and averaging all such values starting from $t_f = 1000\ \tau$ (4 ps). This averaging was done because the function values appear to oscillate aperiodically about an asymptote. We used the same choices of (n_{zero}, n_{inf}) here as for the Green-Kubo calculations.

Radial distribution (pair correlation) functions $g_{BiCl}(r)$ were computed in 0.1 Å bins using visual molecular dynamics software[35] and 54 000 timesteps of data. Coordination numbers of Bi (average number of Cl atoms near Bi) were calculated from the $g_{BiCl}(r)$ using Eq. (16):

$$N_{Bi} = \int_0^{rshell} g_{BiCl}(r)\cdot\rho_{Cl}\cdot 4\pi r^2\cdot dr, \tag{16}$$

where ρ_{Cl} = number density ($Å^{-3}$) of Cl atoms in the cell. The integration limit r_{shell} was taken to be 4.0 Å (the location of the first minimum of the integrand). We also defined a "tight coordination number" (TN_{Bi}), using the same equation but choosing $r_{shell} = 2.7$ Å, as a crude metric for the number of Cl atoms that were bound to only one Bi atom. By stoichiometry, the coordination numbers of Cl atoms (N_{Cl}, TN_{Cl}) are simply 1/3 of the Bi values (N_{Bi}, TN_{Bi}).

III. RESULTS

A. Specific conductivity σ

Figure 3 plots running-integral results for the Green-Kubo computations of D_{Cl}, D_{Bi}, and σ. The short-range numerical noise (best seen in the left-side plots which have more points) increases from $D_{Cl} \rightarrow D_{Bi} \rightarrow \sigma$ because the amount of data per time step decreases: $48 \rightarrow 16 \rightarrow 1$. Theoretically the curves in these six plots should have horizontal asymptotes, although this is only clear in the chlorine diffusion integrals (top row of plots); these curves must be prone to slow and

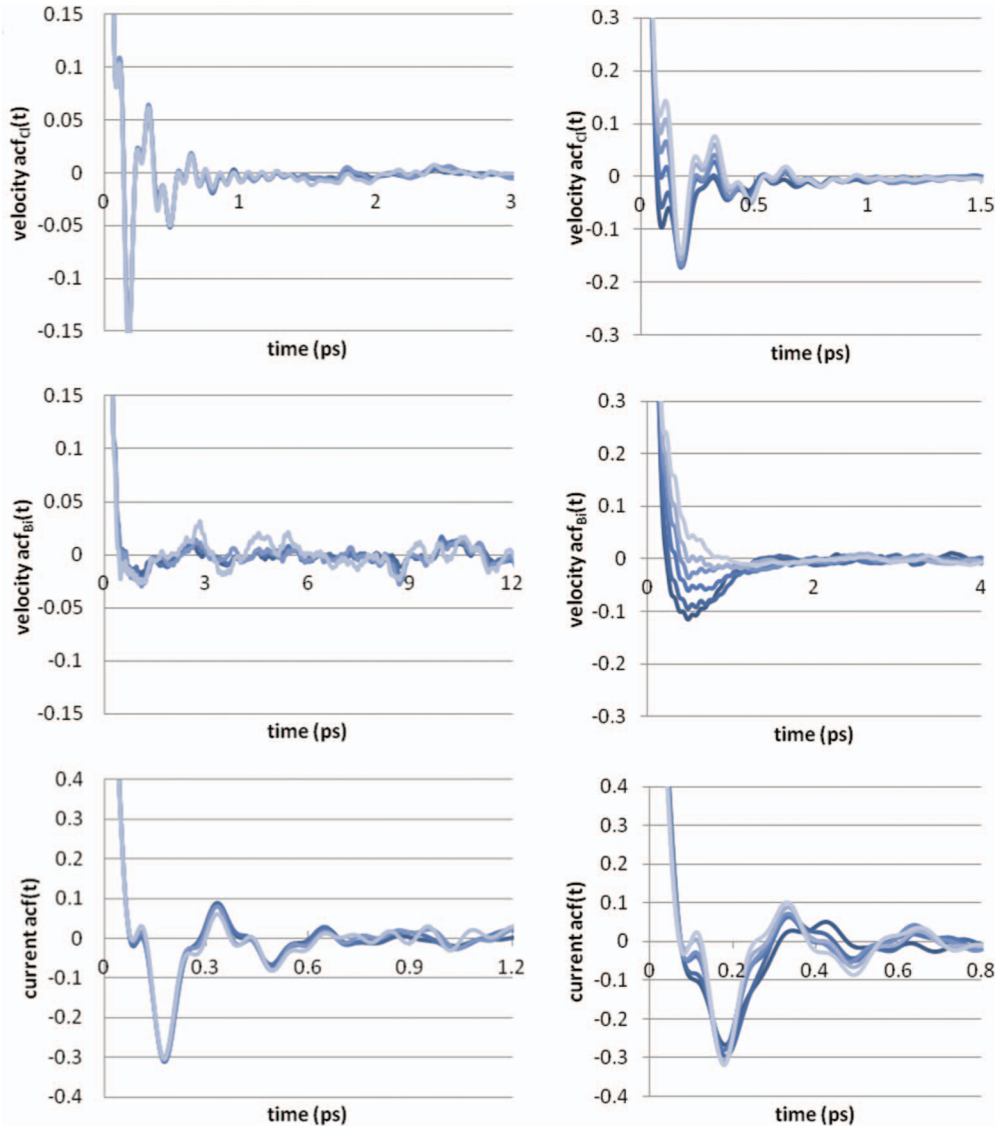

FIG. 2. Normalized autocorrelation functions for $BiCl_3$. Left set: At 580 °C, showing effects of function averaging over choices of time zero (from light to dark: 8000, 18 000, 28 000, 38 000 choices). Right set: Using only the most accurate 38 000-t_0-averaged functions, showing effects of temperature (from light to dark: 660, 580, 500, 420, 340, 260 °C). Note the persistent oscillations (~10 per ps) due to Cl vibrations (~300 cm^{-1}) in all plots.

random oscillations ("wandering") about asymptotic values. The left-side plots show a bit less of this random long-range oscillation when more accurate functions (from increased function averaging, darker curves) are used. Gratifyingly, despite the uncertainties in asymptote derivation, the conductivity integrals (bottom right plot) do appear to give the largest values for intermediate temperatures, in agreement with the experimentally observed conductivity maximum versus temperature.

Figure 4 plots running-limit results for the Einstein computations of the same properties. The left-side plots show much less short-range noise than in the Green-Kubo computations of Fig. 3, and although there are long-range oscillations, they are in Fig. 4 somewhat improved from their Fig. 3 counterparts. A nice barometer of the precision of results was the smoothness of the resulting D_{Bi} values (Table I): fits of our results to a simple 2nd order polynomial in T revealed that D^{Ein} outperformed D^{GK} for all choices of (n_{zero}, n_{inf}), and that the use of (n_{zero}, n_{inf}) = (38k, 16k) gave near-perfect fits with either D^{Ein} or D^{GK}. Only results from using (n_{zero}, n_{inf}) = (38k, 16k) will be presented below.

Table II presents results from the most efficient use of our data. The most important result here is that the conductivity estimates σ^{GK} and σ^{Ein} qualitatively reproduce the experimental phenomenon of a maximum versus temperature. As expected from observations above, the σ^{Ein} values appear to be somewhat more precise than σ^{GK} values, resulting in a smoother dependence upon T. The values are 2 to 4 times larger than σ^{expt}, which we suspect is due to Bi-Cl attractive forces being slightly underpredicted by the non-relativistic Born-Oppenheimer density functional theory approximation used in the simulation. Considering that the ~10^{-6} Ω^{-1} cm^{-1}conductivity of molten $SbCl_3$ [36] is 500 000 times smaller than that of $BiCl_3$, the level of agreement with experiment here seems quite satisfactory. Since the AIMD simulations have proved to be successful in qualitatively reproducing the maximum, they can be further analyzed to find reasons for this maximum.

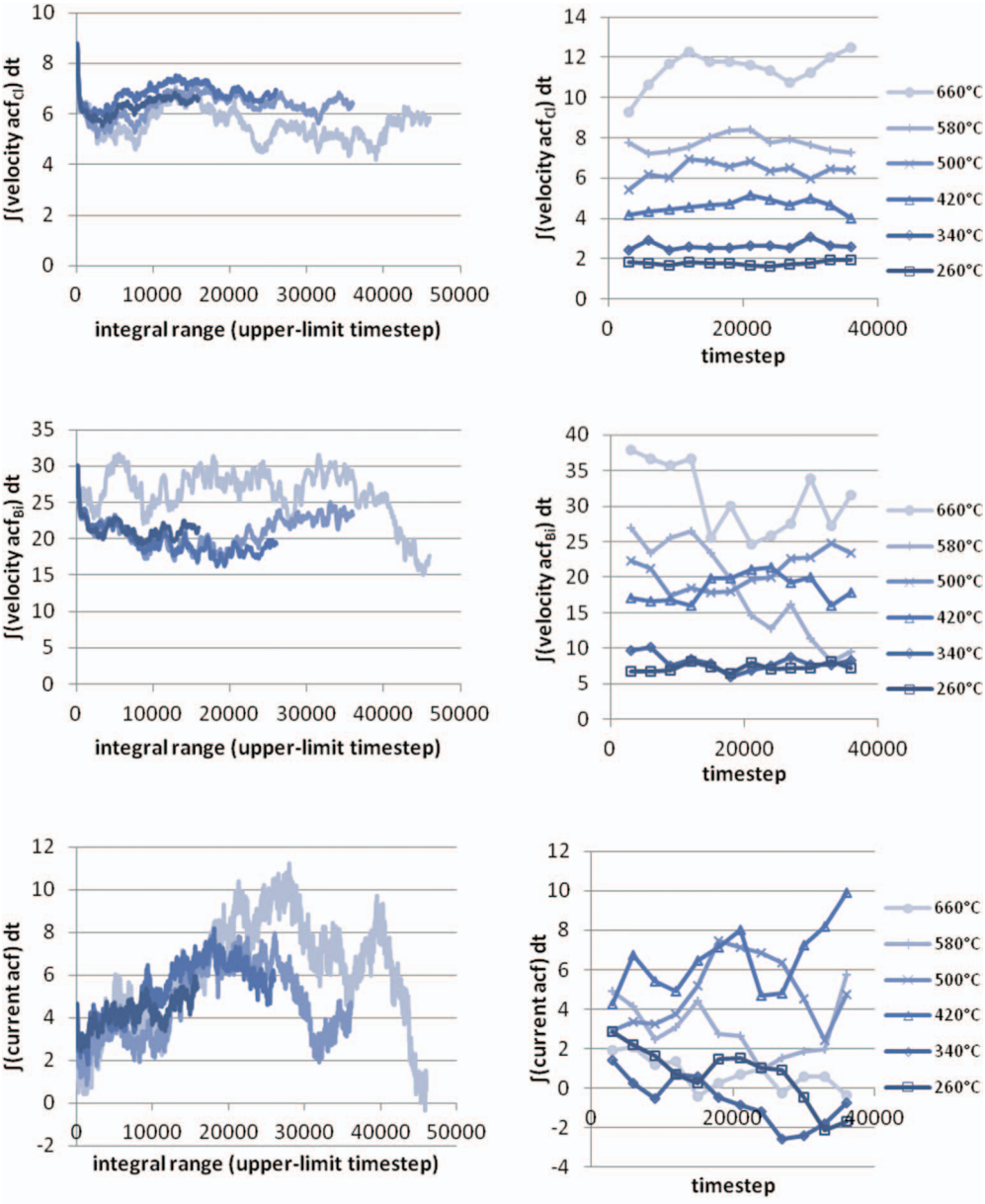

FIG. 3. Running integrals of normalized autocorrelation functions for $BiCl_3$. Left set: at 500 °C, showing effects of function averaging over choices of time zero (from light to dark: 8000, 18 000, 28 000, 38 000 choices). Right set: data from 18 000-t_0-averaged functions, showing effects of temperature. The values are seen to wander about their theoretical asymptotes. Despite the uncertainty in determining asymptotic values, conductivities (bottom right plot) are noticeably largest for the midrange temperatures (420 and 500 °C), as observed experimentally.

Also in Table II, the computed diffusion coefficients D_{Bi} and D_{Cl} are seen to rise continuously with temperature, which forces the Nernst-Einstein values for specific conductivity (σ^{NE}) to also rise continuously with temperature, leading to increasingly poorer Haven ratios. Clearly, correlation of motion of ions of opposing charge is occurring and increasing with T. Nernst-Einstein errors of ~20% were seen for alkali halides long ago,[29] but here the problems with this approximation are significantly worse.

It had been believed that the conductivity maximum under orthobaric conditions was due primarily to changes in density rather than temperature, since the maximum goes away at high pressures which minimize density changes.[5,7,37] Density effects are more complex than had been thought. In our second set of runs, a 260 °C simulation was run at the density of the 580 °C run, and vice versa (Table III). The diffusion constants show a dependence on both T and ρ: diffusion is enhanced by warmer temperatures and reduced densities. The conductivity trends are more interesting: as the density was jumped from 3.11 to 3.85 g ml^{-1}, conductivity *rose* at cold T but *fell* at high T. This complex behaviour was an important clue for deciphering the underlying Arrhenius relation for $BiCl_3$ conductivity (see Sec. III C).

B. Coordination numbers

The observed coordination numbers of bismuth atoms (N_{Bi}) in the simulated melt were not the expected 2 to 4 from Tödheide's hypothetical equilibrium, but 5.7 to 6.8 (Table IV). The number is 3 in the gas[38] and a "frustrated" 8 in the crystal[39] (three Cl atoms at 2.5 Å, the next five at 3.2–3.4 Å). The radial distribution functions (Fig. 5) show,

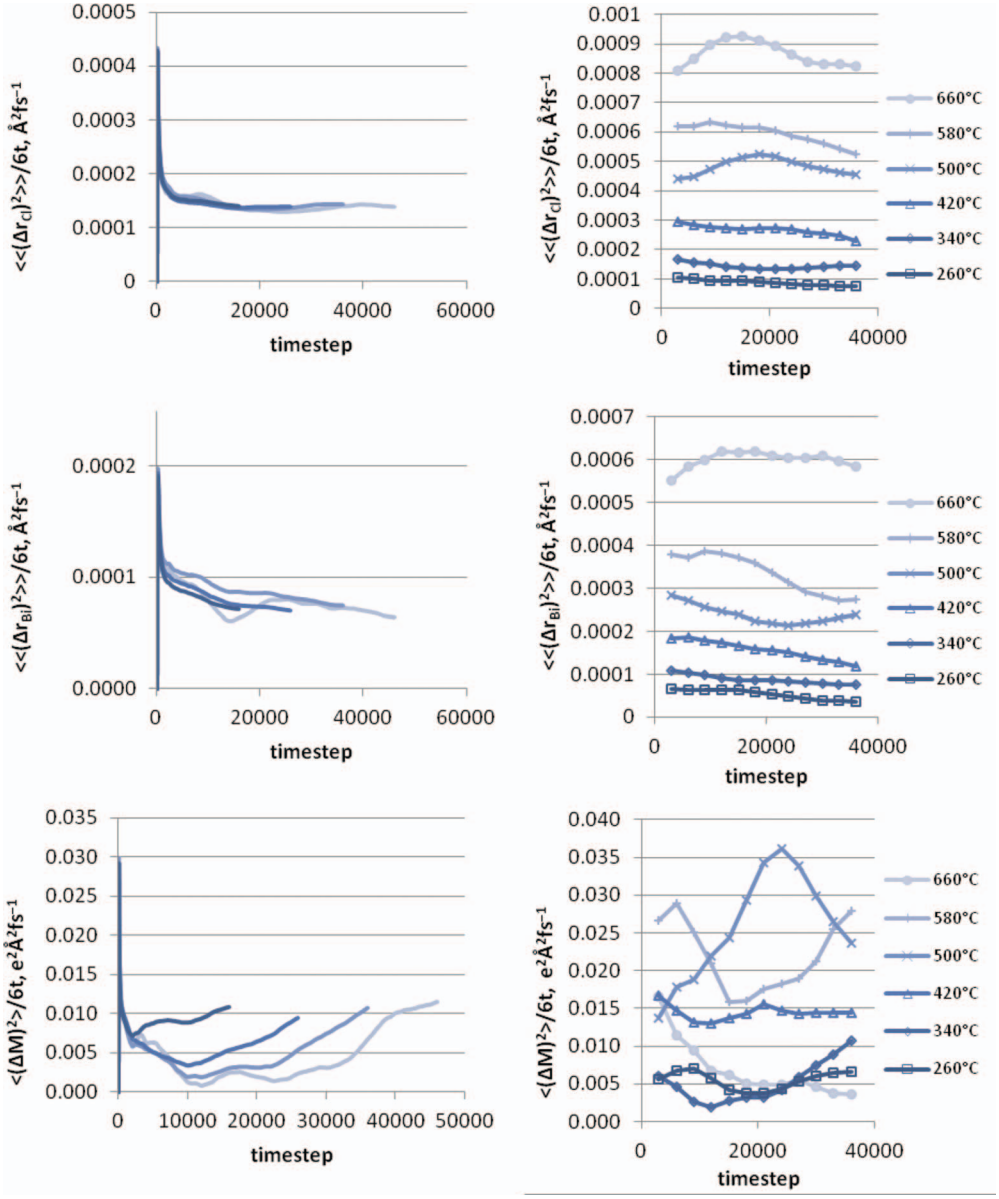

FIG. 4. Einstein-style functions for $BiCl_3$ (see Eq. (13) and (14)). Left set: at 340 °C, showing effects of function averaging over choices of time zero (from light to dark: 8000, 18 000, 28 000, 38 000 choices). Right set: data from 18 000-t_0-averaged functions, showing effects of temperature. Both the long-range wandering about their theoretical asymptotes and the short-range noise is reduced here compared to Green-Kubo computations (Fig. 3). Conductivities here (bottom right plot) again show largest values for midrange temperatures (500 and 580 °C).

as temperature increases, a distribution of nearest Cl atoms that becomes increasingly L-shaped, with more Cl atoms at a 2.6 Å covalent position. The simulation movies revealed *all* Cl atoms spending substantial times bridging two Bi atoms, but also frequently migrating to new interbismuth areas via brief periods of single-Bi coordination, on a picosecond timescale. At the hotter temperatures, there were clearer instances of Cl atoms periodically behaving as non-bridging, covalently bound Cl atoms (1-coordinate Cl atoms), vibrating between 2.4 and 2.6 Å.

TABLE I. R^2 values from parabolic fits of D_{Bi} (from AIMD simulations) versus temperature.

(n_{zero},n_{inf})	R^2 (D_{Bi}^{Ein})	R^2 (D_{Bi}^{GK})
(38, 16)	1.000	0.999
(28, 26)	0.997	0.968
(18, 36)	0.983	0.919
(8, 46)	0.982	0.901

With the absence of identifiable molecular ions, what, then, are the conducting ions in this liquid? Is there still an identifiable ion-association equilibrium for which a degree-of-ionization theory may still be applied? We tested the most logical idea left to us by the simulations: that the conductivity is due to mobile Cl^- ions moving against (and exchanging with) large networks of $Bi_xCl_y^{z+}$ clusters. We considered an equilibrium between mobile ("ionic") and locked ("covalent") chloride ions, and as a distinguishing criterion we considered immobile chlorides be those within 2.7 Å of a Bi atom, since in almost all of these instances (except perhaps at the coldest temperatures) these Cl atoms are essentially "locked" onto and vibrating against one Bi atom. Table IV

TABLE II. Diffusion coefficients D and specific conductivity σ from AIMD simulations.

T (°C)	ρ[a] (g cm^{-3})	$D_{Bi}^{Ein}/10^{-10}$ (m^2 s^{-1})	$D_{Cl}^{Ein}/10^{-10}$ (m^2 s^{-1})	σ^{expt} [b] (Ω^{-1} cm^{-1})	σ^{Ein} (Ω^{-1} cm^{-1})	σ^{GK} (Ω^{-1} cm^{-1})	σ^{NE} (Ω^{-1} cm^{-1})	Haven ratio[c]
260	3.8468	4.9	8.5	0.433	0.9	1.0	1.8	2.1
340	3.6628	8.2	15.0	0.551	1.2	0.3	2.5	2.1
420	3.4788	15.0	25.9	0.585	1.5	2.1	3.8	2.6
500	3.2948	24.7	44.2	0.556	2.0	2.2	5.4	2.7
580	3.1108	37.9	61.2	0.489	1.8	1.5	6.8	3.8
660	2.9268	53.7	81.6	0.404	0.8	0.5	8.1	9.7

[a]Density employed in the simulations, from Eq. (6).
[b]Interpolated from data of Grantham and Yosim Ref. 2.
[c]Computed as σ^{NE}/σ^{Ein}.

reveals that these tight coordination numbers TN_i generally increase with temperature, in opposition to the regular N_i values, and in agreement with the Yosim hypothesis that there is increasing ion association as T increases. However, assuming TN_{Cl} to be a weighted average of 0 (mobile Cl) and 1 (locked Cl)

$$TN_{Cl} = (\alpha)0 + (1-\alpha)1 \tag{17}$$

the degree of ionization α takes on rather small values of 0.15–0.22, much lower than the values Tödheide derived from the erroneous assumptions of heavier $BiCl_x$ ions and monotonically rising ion mobilities. When the experimentally measured conductivities are back-corrected for this mild effect of degree of ionization via Eq. (4), the resulting mobilities of mobile chloride (Table IV) do not monotonically rise with temperature, but exhibit a maximum.

How can ion mobilities go through a maximum if their diffusion coefficients do not? The answer is that the absolute diffusion constants are related to absolute mobility, but Eqs. (1)–(4) require *relative* mobility of cations against anions. Equation (1) fails for molten salts for the same reason that the Nernst-Einstein approximation does: cation and anion motions are not sufficiently independent, and hence relative and absolute mobilities cannot be equated. Given the difficulty in expressing a relative mobility, the difficulty in attempting to define a degree of ionization in this liquid, and considering that Tödheide himself admitted an ambiguity in separating α from μ_i in the case of molten lithium halides,[7] we feel that the degree-of-ionization theory is inappropriate. A new theory is needed.

C. New theory, and least-squares fits

Molten $BiCl_3$ is composed of atomic ions. The temperature dependence of its conductivity can be expressed as an ordinary Arrhenius relation if both the frequency factor A and the activation energy E_a are expressed as functions of density

$$\sigma(T,\rho) = A(\rho)e^{-E_a(\rho)/kT}. \tag{18}$$

Unlike hole theory, in which activation energies relate to formation of suitably sized holes[40] and has been criticized,[7,37,40] we consider the activation energy to be the energy needed for an ion to hop from counter-ion to counter-ion, e.g., Cl^- to hop from one Bi^{3+} to another, or Bi^{3+} to hop from one Cl^- to another (Fig. 6). Hence, the exponential term corresponds to the probability that a hop will be successful, and *rises* with rising density because of the reduced hopping distances which lower E_a. The frequency factor A corresponds to the total number of potential hops available to the set of ions at a given time, but this *falls* with rising liquid density because of increased crowding which restricts hopping opportunities. These competing effects result in a conductivity maximum versus density at constant temperature; in $BiCl_3$ the optimal density is near $\rho = 3.5$ g ml^{-1}. In the orthobaric experiments of Grantham and Yosim,[2–5] density and temperature are linearly correlated, and the maximum versus temperature observed in their work is simply the maximum versus density but plotted against the experimentally controllable parameter, as we demonstrate below.

The dependence of E_a upon ρ is derived as follows. Suppose an anion (charge q_2) is hopping between two cations (charge q_1) located at $x = x_1$ and $x = x_2$, with x_2-$x_1 = R$. The sum of the two attractive interactions is $E(x) = q_1q_2/4\pi\varepsilon_0(x\text{-}x_1) + q_1q_2/4\pi\varepsilon_0(x_2\text{-}x)$. Then $E_a = E_{max} - E_{min} = E(x_1 + R/2) - E(x_1 + r_0)$, where r_0 is the preferred anion-cation bond length. The result is

$$E_a(\rho) = \frac{|q_1q_2|}{4\pi\varepsilon_0}\left(\frac{R}{r_0(R-r_0)} - \frac{4}{R}\right), \quad R \geq 2r_0, \tag{19}$$

which is dependent upon density because $R = P\rho^{-1/3}$ for some proportionality constant P. E_a is zero when the anion is in contact with both cations ($R = 2r_0$), and E_a approaches its asymptotic maximum $E_{a,max} = |q_1q_2|/4\pi\varepsilon_0 r_0$ as $R\to\infty$, i.e., as $\rho\to 0$. For $BiCl_3$, $q_1 = 3e$, $q_2 = -e$, $r_0 = 2.6$ Å (Fig. 5), and $E_{a,max} = 1603$ kJ mol^{-1}.

TABLE III. Temperature and density effects on D_{Bi}, D_{Cl}, and σ from AIMD simulations.

T (°C)	ρ (g cm^{-3})	D_{Bi}^{Ein}/ 10^{-10} m^2 s^{-1}	D_{Cl}^{Ein}/ 10^{-10} m^2 s^{-1}	σ^{Ein} (Ω^{-1} cm^{-1})
260	3.8468	4.9	8.5	0.9
260	3.1108	10.5	16.7	0.6
580	3.8468	18.2	32.3	1.3
580	3.1108	37.9	61.2	1.8

TABLE IV. Coordination numbers (and derived quantities) from AIMD simulations.

T (°C)	ρ (g cm^{-3})	N_{Bi}	N_{Cl}	TN_{Bi}	TN_{Cl}	α	σ^{expt} [a] (Ω^{-1} cm^{-1})	Λ^{expt} [b] (Ω^{-1} cm^2 mol^{-1})	Ion mobility[c]/10^{-4} (C s kg^{-1})
260	3.8468	6.79	2.26	2.35	0.78	0.22	0.433	35.5	0.56
340	3.6628	6.54	2.18	2.39	0.80	0.20	0.551	47.4	0.81
420	3.4788	6.32	2.11	2.45	0.82	0.18	0.585	53.0	1.01
500	3.2948	6.11	2.04	2.49	0.83	0.17	0.556	53.2	1.09
580	3.1108	5.88	1.96	2.53	0.84	0.16	0.489	49.5	1.09
660	2.9268	5.66	1.89	2.55	0.85	0.15	0.404	43.6	1.00

[a]Interpolated from data of Grantham and Yosim Ref. 2.
[b]Derived from σ^{expt}.
[c]Estimated as $\Lambda^{expt}/3\alpha eN_{AVO}$, Eq. (4).

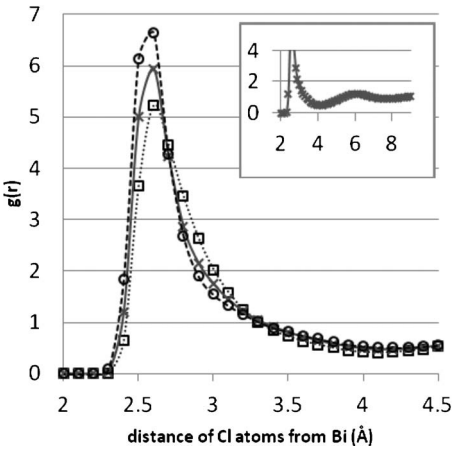

FIG. 5. Radial distribution functions from AIMD simulations. Squares: 340 °C. X's (including inset): 500 °C. Circles: 660 °C.

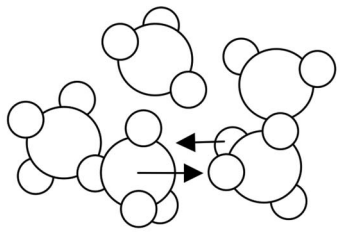

Low density: high A but high E_a

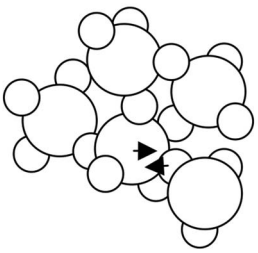

High density: low A but low E_a

FIG. 6. Effect of density upon Arrhenius parameters for conductivity.

The dependence of A upon ρ is unknown. To minimize the number of fitting parameters, we used a simple linear relationship

$$A(\rho) = A_0 - A_1\rho \tag{20}$$

with A_0 and A_1 used as fitting parameters.

For commonly one-dimensional experiments in which ρ = f(T) (see Eq. (6) for $BiCl_3$), Eq. (18) can be reduced to a one-dimensional temperature-dependent expression by substituting this f(T) for ρ in Eqs. (19) and (20). We used Eq. (6) for this purpose, to fit Eq. (18) to the 22 points plotted by Grantham and Yosim,[2] varying only the parameters {A_0, A_1, P}. The fit was quite good, with an rms error of less than 2% (0.005 Ω^{-1} cm^{-1}) from the following parameter values: A_0 = 4.012 Ω^{-1} cm^{-1}, A_1 = 0.9306 Ω^{-1} cm^2 g^{-1}, and P = 8.18 Å g$^{1/3}$ cm. The resulting functions $E_a(\rho)$ and $A(\rho)$ in Eqs. (19) and (20) are plotted in Fig. 7. The A values are near 1 Ω^{-1} cm^{-1} and the E_a values are below 8 kJ mol^{-1}, both comfortably commensurate with the relatively high conductivity of this liquid.

Other Arrhenius-like relations have been used by others for fitting to various transport properties of liquids (y = viscosity η, conductivity σ, etc.). Below are four examples:[40–44]

$$y_{ARR} = Ae^{B/RT} \quad \text{(Arrhenius)}, \tag{21}$$

$$y_{LIT} = Ae^{B/RT^3} \quad \text{(Litovitz)}, \tag{22}$$

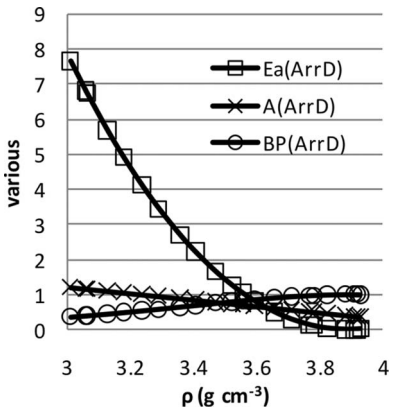

FIG. 7. Results for Arrhenius parameters A (Ω^{-1} cm^{-1}) and E_a (kJ mol^{-1}) after least-squares fitting of the new conductivity function to experimental data of Ref. 2. BP is the Boltzmann probability $e^{-Ea/RT}$ using Eq. (6) for the relevant orthobaric temperatures.

$$y_{VFT} = Ae^{B/R(T-T_0)} \quad \text{(Vogel} - \text{Fulcher} - \text{Tammann)}, \tag{23}$$

$$y_{DOR} = A_1 e^{B_1/RT} + A_2 e^{B_2/RT} \quad \text{(Doremus)}. \tag{24}$$

All A and B constants are assumed independent of density. The four-parameter function of Doremus is newest and arose from his observation[43] that the Arrhenius plot (ln η vs. 1/T) for the viscosity of silica over a large temperature range exhibits two different linear regions with two differing slopes, connected by a kink in the plot. Such a situation is not fit as well by Litovitz or VFT equations, and Doremus went on to fit viscosities of several molten silicates with his new function.[45] Both Doremus[43,45] and Ojovan and Lee[46] took B_1 and B_2 in η_{DOR} to be constant activation energies; one for creating defects (breaking bonds), and the other for motion of defects (or fragmented atoms or groups of atoms from the network). In fact, the orthobaric viscosities of $BiCl_3$ also exhibit a Doremus-style kinked linear plot, as Kellner showed over 40 years ago;[47] he used the two slopes to determine activation energies of 4.8 and 3.4 kcal mol^{-1}.

However, specific conductivity and viscosity can have quite different temperature dependence, and for $BiCl_3$, although η monotonically decreases with T and has a kinked linear Arrhenius plot, σ shows a maximum with T and has a curved Arrhenius plot with no linear regions. Kellner made the relevant comment that viscosity relates more to the mobility of the largest ion, while conductivity relates more to the mobility of the smallest ion.[47] Thus, the Doremus equation or extensions[48] may not be appropriate for molten salt conductivity. The LIT and VFT equations are currently popular for fitting conductivities of room-temperature ionic liquids.[42,49]

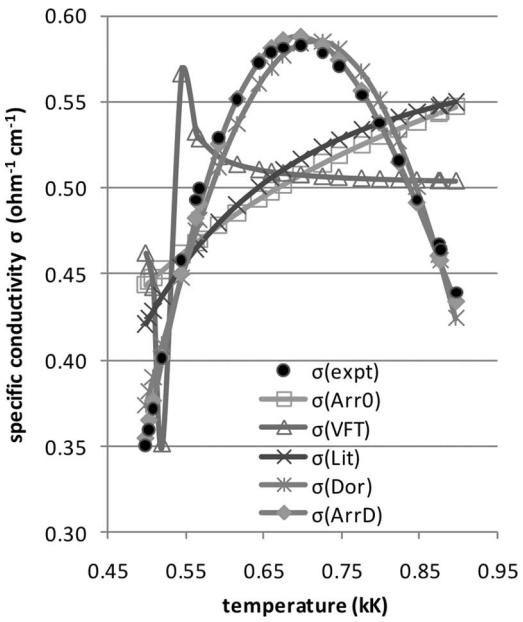

FIG. 8. Fits to experimental $BiCl_3$ conductivities of Ref. 2, showing superiority of the ArrD function over others.

We applied these four Eqs. (21)–(24) to σ of $BiCl_3$ (Fig. 8). The ARR, LIT, and VFT functions are incapable of producing a maximum. The DOR function can produce a maximum but the fit is visibly poorer than that of the density-dependent Arrhenius function ("ArrD," Eq. (18)), despite having an extra fitting parameter (4 vs. 3).

Further support for the ArrD function comes from testing its predictions for other combinations of T and ρ. For (T, ρ) = (260 °C, 3.11 g ml^{-1}) and (580 °C, 3.85 g ml^{-1}) the function predicts 0.29 and 0.43 Ω^{-1} cm^{-1}. The AIMD results σ^{Ein} (Table III) are again 2 to 4 times higher, as expected from the Table I comparison of σ^{Ein} with σ^{expt}. Most importantly, the ArrD function correctly predicts the qualitative observation made from this simulation data: as ρ is jumped from 3.11 to 3.85 g ml^{-1}, σ rises at 260 °C but falls at 580 °C. If ρ were varied continuously, a maximum would be observed at both temperatures: (ρ, σ) = (3.55, 0.546) at 260 °C, and (3.45, 0.617) at 580 °C.

IV. CONCLUSIONS

Molten bismuth chloride is composed of atomic ions, rather than a molecular liquid containing $BiCl_2^+$ and $BiCl_4^-$ ions as previously assumed by Tödheide.[6,7] A new attempt to apply degree-of-ionization theory to discrete categorizations of mobile versus immobile chloride ions did not work. Instead, the conductivity maximum is concluded to be due to a maximum in relative ion mobility in the melt, rather than a balance between rising mobility and decreasing ionization. Diffusion coefficients for Bi and Cl relate to absolute (not relative) ion mobility, mask the strong correlations of cation/anion motion, and lead to disastrous Nernst-Einstein predictions for conductivity.

A new theory is presented. It is suggested that Cl and Bi ions conduct electricity by hopping from counterion to counterion, with frequency factors A and activation energies E_a that both fall with increasing liquid density. These competing effects give rise to the conductivity maximum. Least-squares fitting showed that the ordinary Arrhenius equation, with ρ-dependent A and E_a, fits experimental results to within 2%, better than modified Arrhenius relations traditionally used. The new theory is expected to apply to other molten salts as well.

ACKNOWLEDGMENT

We gratefully acknowledge Natural Sciences and Engineering Research Council (NSERC), Canada for operational grant funding and CFI, Government of Saskatchewan, and CiaraTech (Canada) for supercomputer funding. J. Jorgenson (Laboratory of Computational Discovery, Regina) is thanked for system and software assistance. G. Hanna (University of Alberta) and G. Patey, M. Thachuk, and D. Luckhaus (University of British Columbia) are thanked for valuable discussions.

APPENDIX: DERIVATIONS OF EQS. (9) AND (14)

For estimation of specific conductivity, the more common forms of the Green-Kubo[37] and Einstein[50] formulae are

$$\sigma^{GK} = (3VkT)^{-1}\int_{t=0}^{\infty}\langle C_J(t;t_0)\rangle dt,$$
$$C_J(t;t_0) = \vec{j}(t)\bullet\vec{j}(t_0), \tag{A1}$$

$$\sigma^{Ein} = \frac{1}{VkT}\lim_{t\to\infty}\frac{\langle|\vec{M}(t)-\vec{M}(t_0)|^2\rangle}{6t}, \tag{A2}$$

where the brackets indicate averaging over time variable t_0. Normalizing $C_J(t; t_0)$,

$$\sigma^{GK} = \frac{\langle\vec{j}^2(t_0)\rangle}{3VkT}\int_{t=0}^{\infty}\frac{\langle C_J(t;t_0)\rangle}{\langle\vec{j}^2(t_0)\rangle}dt$$
$$\sigma^{GK} = \frac{\langle\vec{j}^2\rangle}{3VkT}\int_{t=0}^{\infty}\tilde{C}_J(t;t_0)dt. \tag{A3}$$

Now, Eq. (A2) → (14) and Eq. (A3) → (9) because

$$\langle\vec{j}^2\rangle = 3nkT\Theta, \tag{A4}$$

which is shown below.

$$\langle\vec{j}^2\rangle = \left\langle\left(\sum_i^{Nions} z_i e\vec{v}_i(t_0)\right)\bullet\left(\sum_i^{Nions} z_i e\vec{v}_i(t_0)\right)\right\rangle$$
$$\langle\vec{j}^2\rangle = e^2\sum_i^{Nions} z_i^2\langle\vec{v}_i^2\rangle + 2e^2\sum_i^{Nions}\sum_{j>i}^{Nions} z_i z_j\langle\vec{v}_i\bullet\vec{v}_j\rangle. \tag{A5}$$

Assuming the double sum of cross terms to be negligible, we focus on the sum of diagonal terms and separate it by species

$$\langle\vec{j}^2\rangle = e^2\left(\sum_i^{n_A} z_A^2\langle\vec{v}_{A,i}^2\rangle + \sum_i^{n_B} z_B^2\langle\vec{v}_{B,i}^2\rangle\right)$$
$$\langle\vec{j}^2\rangle = e^2\left(n_A z_A^2\frac{3kT}{m_A} + n_B z_B^2\frac{3kT}{m_B}\right),$$

since $\frac{1}{2}m\langle v^2\rangle = \frac{3}{2}kT$. If n is the number of formula units A_xB_y in the sample cell, then $n_A = -z_B n$, $n_B = z_A n$, and

$$\langle\vec{j}^2\rangle = 3nkTe^2\left(\frac{-z_A^2 z_B}{m_A} + \frac{z_A z_B^2}{m_B}\right),$$

which matches Eq. (A4). Values of $\langle\vec{j}^2\rangle$ explicitly computed from simulations via Eq. (A5) matched the Eq. (A4) predictions within 2.1% (Table V).

TABLE V. Values of $\langle j^2\rangle$ from AIMD simulations (Eq. (A5)) and predicted (Eq. (A4)).

T (°C)	$\langle j^2\rangle_{Eq.(A5)}/10^{-31}$ (C^2 m^2 s^{-2})	$\langle j^2\rangle_{Eq.(A4)}/10^{-31}$ (C^2 m^2 s^{-2})
260	6.99	6.97
340	7.92	8.02
420	8.98	9.07
500	9.93	10.11
580	11.32	11.16
660	11.95	12.21

[1] M. Galinski, A. Lewandowski, and I. Stepniak, Electrochim. Acta **51**, 5567 (2006).
[2] L. F. Grantham and S. J. Yosim, J. Phys. Chem. **67**, 2506 (1963).
[3] L. F. Grantham and S. J. Yosim, J. Chem. Phys. **45**, 1192 (1966).
[4] L. F. Grantham and S. J. Yosim, J. Phys. Chem. **72**, 762 (1968).
[5] A. J. Darnell, W. A. McCollum, and S. J. Yosim, J. Phys. Chem. **73**, 4116 (1969).
[6] G. Treiber and K. Tödheide, Ber. Bunsenges. Phys. Chem. **77**, 540 (1973).
[7] K. Tödheide, Angew. Chem., Int. Ed. Engl. **19**, 606 (1980).
[8] J. T. Kenney and F. X. Powell, J. Phys. Chem. **72**, 3094 (1968).
[9] E. Denchik, S. C. Nyburg, G. A. Ozin, and J. T. Szymanski, J. Chem. Soc. A **1971**, 3157.
[10] K. W. Fung, G. M. Begun, and G. Mamantov, Inorg. Chem. **12**, 53 (1973).
[11] D. L. Price, M.-L. Saboungi, W. S. Howells, and M. P. Tosi, in *Proceedings of Internation Symposium on Molten Salts*, edited by M.-L. Saboungi *et al.* (The Electrochemical Society PV 93-9, Pennington, NJ, 1993), p. 1.
[12] When $\alpha = 1$, a plot of σ versus p (constant T) has a conductivity maximum, due to competing effects of μ vs. V_m in Eq. (3); both mobility and molar volume are decreasing. This maximum appears at high pressures, however (~2 kbar for NaCl at 900 °C, see Ref. 7), and is not important to the orthobaric $BiCl_3$ experiments where both σ and Λ exhibit conductivity maxima.
[13] S. J. Yosim, A. J. Darnell, W. G. Gehman, and S. W. Mayer, J. Phys. Chem. **63**, 230 (1959).
[14] C. G. Maier, U.S. Bureau of Mines Technical Paper 360 (1925).
[15] J. W. Johnson and D. Cubicciotti, J. Phys. Chem. **68**, 2235 (1964).
[16] C. A. Kraus, Phys. Rev. (Series I) **18**, 40 (1904).
[17] C. A. Kraus, Phys. Rev. (Series I) **18**, 89 (1904).
[18] G. Kresse and J. Hafner, Phys. Rev. B **47**, 558 (1993).
[19] G. Kresse and J. Furthmüller, Phys. Rev. B **54**, 11169 (1996).
[20] G. Kresse and J. Hafner, J. Phys.: Condens. Matter **6**, 8245 (1994).
[21] G. Kresse and D. Joubert, Phys. Rev. B **59**, 1758 (1999).
[22] S. Nosé, J. Chem. Phys. **81**, 511 (1984).
[23] A. R. Leach, *Molecular Modelling: Principles and Applications*, 2nd ed. (Pearson, Harlow, UK, 2001).
[24] J. P. Perdew, J. A. Chevary, S. H. Vosko, K. A. Jackson, M. R. Pedersen, D. J. Singh, and C. Fiolhais, Phys. Rev. B **46**, 6671 (1992).
[25] S. Grimme, J. Comp. Chem. **27**, 1787 (2006).
[26] G. J. Janz, J. Phys. Chem. Ref. Data **17** (Suppl. 2) (1988).
[27] K. R. Harris, J. Phys. Chem. B **114**, 9572 (2010).
[28] K. Compaan and Y. Haven, Trans. Faraday Soc. **54**, 1498 (1958).
[29] A. Noda, K. Hayamizu, and M. Watanabe, J. Phys. Chem. B **105**, 4603 (2001).
[30] K. Ueno, H. Tokuda, and M. Watanabe, Phys. Chem. Chem. Phys. **12**, 1649 (2010).
[31] N. A. Stolwijk and S. Obeidi, Electrochim. Acta **54**, 1645 (2009).
[32] J. P. Hansen and I. R. McDonald, Phys. Rev. A **11**, 2111 (1975).
[33] T. Frömling, M. Kunze, M. Schönhoff, J. Sundermeyer, and B. Roling, J. Phys. Chem. B **112**, 12985 (2008).
[34] D. R. MacFarlane, M. Forsyth, E. I. Izgorodina, A. P. Abbott, G. Annat, and K. Fraser, Phys. Chem. Chem. Phys. **11**, 4962 (2009).
[35] W. Humphrey, A. Dalke, and K. J. Schulten, J. Mol. Graphics **14**, 33 (1996).
[36] C. Petrovic, G. Mamantov, M. Sørlie, M. H. Lietzke, and G. P. Smith, J. Phys. Chem. **86**, 4598 (1982).
[37] N. H. Nachtreib, Annu. Rev. Phys. Chem. **31**, 131 (1980).
[38] H. A. Skinner and L. E. Sutton, Trans. Faraday Soc. **35**, 681 (1940).
[39] S. C. Nyburg, G. A. Ozin, and J. T. Szymanski, Acta Crystallogr., Sect. B: Struct. Crystallogr. Cryst. Chem. **27**, 2298 (1971).

[40]T. A. Litovitz, J. Chem. Phys. **20**, 1088 (1952).
[41]S. I. Smedley, *The Interpretation of Ionic Conductivity in Liquids* (Plenum, New York, 1980).
[42]M. Kanakubo, K. R. Harris, N. Tsuchihashi, K. Ibuki, and M. Ueno, Fluid Phase Equilib. **261**, 414 (2007).
[43]R. H. Doremus, J. App. Phys. **92**, 7619 (2002).
[44]Doremus (Ref. 43) wrote his equation as $\eta = Ae^{B/RT}[1 + Ce^{D/RT}]$, which is equivalent to Eq. (24) if $A_1 = A$, $A_2 = AC$, $B_1 = B$, and $B_2 = B + D$.
[45]R. H. Doremus, Am. Ceram. Soc. Bull. **82**, 59 (2003).
[46]M. I. Ojovan and W. E. Lee, App. Phys. **95**, 3803 (2004).
[47]J. D. Kellner, J. Phys. Chem. **72**, 1737 (1968).
[48]M. I. Ojovan, K. P. Travis, and R. J. Hand, J. Phys.: Condens. Matter **19**, 415107 (2007).
[49]M. H. Ghatee, M. Zare, A. R. Zolghard, and F. Moosavi, Fluid Phase Equilib. **291**, 188 (2010).
[50]D. Coslovich, J.-P. Hansen, and G. Kahl, J. Chem. Phys. **134**, 244514 (2011).